3rd International Conference on Mechanical Models in Structural Engineering
CMMoST 2015
24-26 June 2015 Seville SPAIN

Damage assessment in a reinforced concrete pedestal based on rotating machinery vibration analysis

Erik Rosado Tamariz[1], Alberto López López[1], David Porras-Navarro González[1]

[1]*Civil Engineering Department, Instituto de Investigaciones Eléctricas (México).*
erosado@iie.org.mx, alopezl@iie.org.mx, david.porras@iie.org.mx

ABSTRACT

A critical operational condition to be considered in the fatigue damage evaluation in reinforced concrete pedestals of power plants generation is the caused by the dynamic effects transmitted by the turbo-generator in terms of vibrations. The structural behavior of the turbo-generator under dynamics conditions is affected by its dimensional characteristics, the weight of each components and the performance of each supports on terms of stiffness and damping.

In this study, a coupled finite element model FEM of the turbo-generator and reinforced concrete pedestal were developed in order to evaluate the dynamic behavior of the structure and the fatigue damage for different real operational conditions according to data obtained from field measurements. The FEM developed for the pedestal considers the inclusion of reinforcing steel structural elements within the concrete. The methodology was implemented to determine the critical zones to fatigue failure and an estimate of remaining fatigue life in the pedestal.

Keywords: Damage Assessment, Reinforced Concrete, Power Plant Pedestal, Numerical Analysis.

1. INTRODUCTION

As part of its improvements process the Mexican electrical system they carry out different actions, including the modernization of some of the critical components of the power plants generation; with the aim to increase its production, as well as to improve their guaranteed net capacities and the net unit heat consumptions. In addition to this modernization process, it is necessary to assess the effects of these changes in the components that not were modified with respect to the original design of the generating unit and interacting directly with upgraded components.

The study case shown in the present work focuses on the evaluation of the dynamic behavior and the estimation of remaining fatigue life in the reinforced concrete pedestal of an upgraded steam turbine for the unit generation of simple cycle as part of its retrofit process. The system analyzed in this study consists of a reinforced concrete pedestal that supports the turbo-generator of the unit generation through eight radial supports and a support of axial type.

The reinforced concrete pedestal of the turbo-generator is formed by a rigid structural system of reinforced concrete frames, which has six bays on the east-west direction and one bay on the north-south direction; the dimensions of length and width of structure are 51.50m and 16.50m respectively,

with three levels of main floor. Since manufacturing and structural drawings [1], the 3D CAD model was developed using commercial CAD software "SolidWorks". In the Figure 1, shows the global view of the geometrical model for the pedestal. The total mass of the pedestal was verified with respect to data reported in design specifications [2].

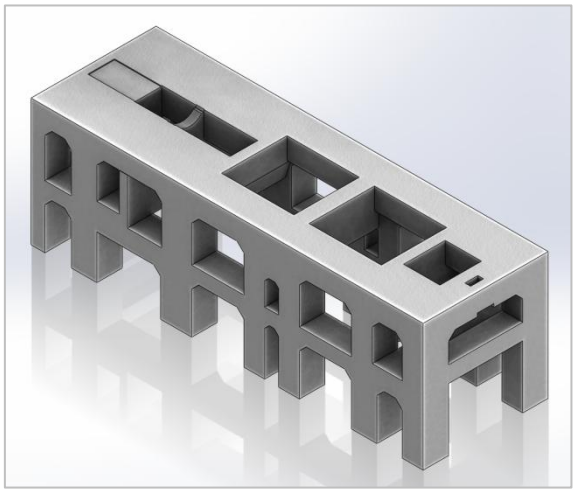

Figure 1. *Geometrical model of the reinforced concrete pedestal.*

Five components comprise the turbo-generator of the generation unit, a rotor of a high pressure (HP), the first rotor of low-pressure turbine (LP1), the Jack Shaft (JS), the second rotor of low-pressure turbine (LP2) and the rotor of electrical generator. Figure 2, shows the distribution and the geometrical model of these components for the turbo-generator.

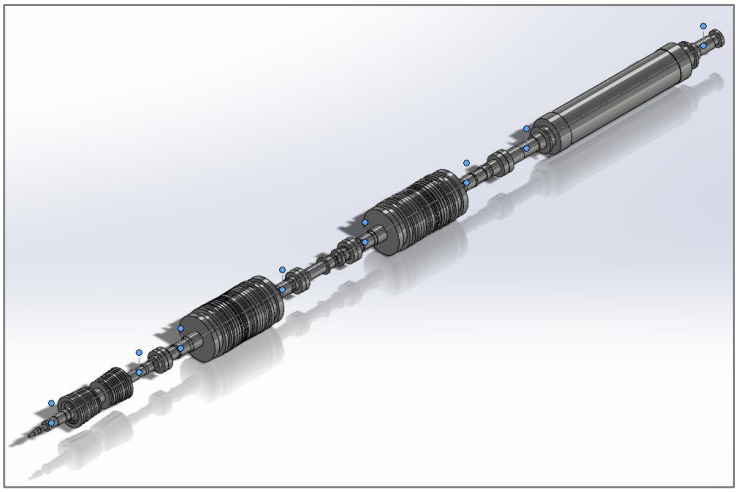

Figure 2. *Distribution and geometrical model of the components that comprise the turbo-generator of the generation unit.*

In order to support the turbo-generator on the reinforced concrete pedestal are used in total nine bearings, of which six are of type cylindrical hydrodynamic located in the high pressure turbine and in the two low pressure turbines, as well as two tilting pads bearings located on the generator. These bearings carry the entire turbo-generator to prevent displacements in the vertical and horizontal directions at the extremities of each turbine and generator. Additionally, there is an axial thrust bearing to prevent displacements along the longitudinal axis at the level of Jack Shaft; which are caused mainly by the sum of the loads at the different stages of the turbines. Figure 3 shows a top

view of the location (in red) of bearings of turbo-generator with respect to concrete pedestal that supports it.

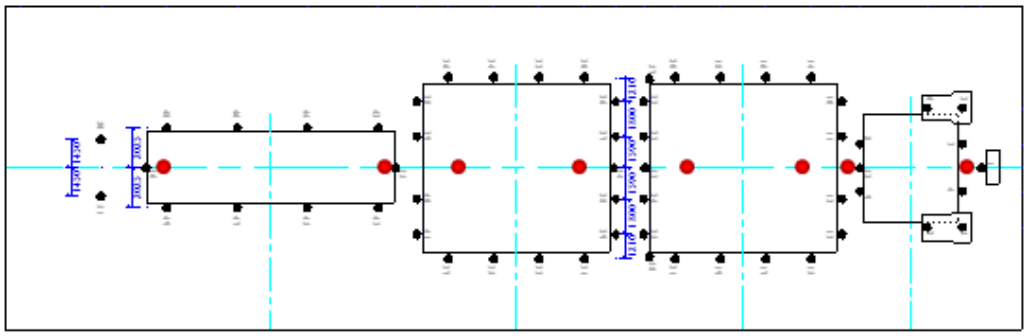

Figure 3. *A top view of the location (in red) of bearings of turbo-generator.*

2. FINITE ELEMENT METHOD

Generally, the finite element stress analysis of a practical engineering component consists of three phases: (a) modeling, (b) analysis, and (c) results interpretation.

Phase I: Modeling

In this phase, which is known as the pre-processing phase, an actual engineering component is represented by an accurate model of a finite element mesh together with specified loading and boundary conditions. The basic aspects for modeling within the finite element method are: (a) element selection, (b) geometrical modeling, (c) material modeling, (d) load modeling, and (e) boundary condition modeling.

Phase II: Analysis

The basic steps of the analysis phase may be summarized as follows:

Step 1: Selection of the field variable models.

In the selection of the field variable models, this step is treated as a separate problem and the field functions (i.e. displacements) inside the element are expressed in terms of nodal displacements and shape functions.

Step 2: Formulation of element stiffness matrices.

The displacements, strains and stresses vectors within each element are derived by using the strain-displacement relationships and Hooke´s law (constitutive equations), it follows that the strains are constant within each element, if the displacements vary linearly. Then, using a variation (energy) formulation, the governing equation for each element is derived.

Step 3: Assembly of the equations for the whole domain.

This step may depend on the type of equation solver employed. In this step the evaluation of element stiffness matrices for all elements in the structure and the assembly of them into the overall stiffness matrix are carried out. This is achieved by adding together contributions of the individual element stiffness matrices and nodal element vectors at common nodes.

Step 4: Application of boundary conditions.

This step results in a reduced system of linear or no-linear equations. The linearity of the equations depends upon the analysis required.

Step 5: Solution of the reduced system of equations.

In this step, either direct or iterative procedures may be employed for the solution of linear systems of equations. The popular direct methods are: the Gauss elimination, Choleskifactorization, and Gauss-Jordan methods, whilst the common iterative solvers are the Gauss-Seidel, and Conjugate Gradient methods.

Phase III. Results Interpretation

This is the post-processing phase, in which the basic interpretation and assessment of finite element results are carried out. Analyst should be aware of the accuracy limitations of finite element results; therefore, results validation or checking out that the results obtained are correct and reliable is an essential step to be considered. The relevant results may be tabulated or represented graphically. Stress contours are advantageous in displaying critical stress-concentration zones. Finite element stress analysis results are usually checked against relevant theories of failure. Figure 4 shows a general scheme for the finite element analysis.

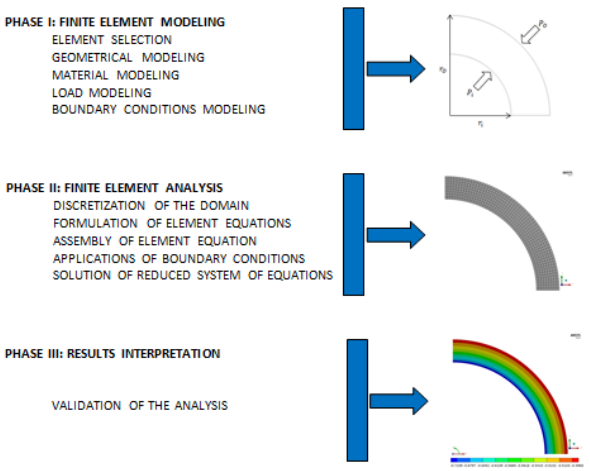

Figure 3. *General scheme of finite element analysis.*

3. DYNAMIC ANALYSIS OF THE STRUCTURE

The dynamic behavior of the turbo-generator and the effects transmitted to the pedestal in terms of vibrations are affected by its dimensional characteristics, the weight of each components and the performance of each supports on terms of stiffness and damping. Therefore, it is important to establish in the numerical analysis of the coupled model, levels of effective stiffness that consider the effects of rotor - bearings - concrete pedestal interaction.

A coupled numerical model of the turbo-generator and reinforced concrete pedestal of a power plant generation was developed in order to evaluate the dynamic behavior of the structure. The numerical model was developed based on the technique of Finite Element Method (FEM) using the commercial code ANSYS [3]. In the dynamic evaluation of the structure were not modeled geometrically and numerically components that do not contribute to the stiffness of the pedestal such as casings, mobile and stationary blades, nozzles and structures of the main bearings. These components were considered as a mass added to the structure.

To simulate the effects of the eight radial bearings that support the turbo-generator, connections coupling for rotor - bearing and bearing - pedestal systems were performed using beam type elements capable of limiting the displacements and rotations so that this element only work in the required direction. Furthermore, the coefficients of stiffness of each element were calibrated with respect to calculated values as reported by the manufacturer on each bearing and each direction were calibrated.

Numerical Model

As a starting point to begin working on dynamic behavior of the structure it was necessary to obtain a 3D CAD model to describe the geometric characteristics of the pedestal and turbo-generator. In the Figures 1 and 2, is shown the details of the 3D CAD models for each component separately. Additionally, in the Figure 4 is shown the 3D geometric coupled model of the turbo-generator and the reinforced concrete pedestal.

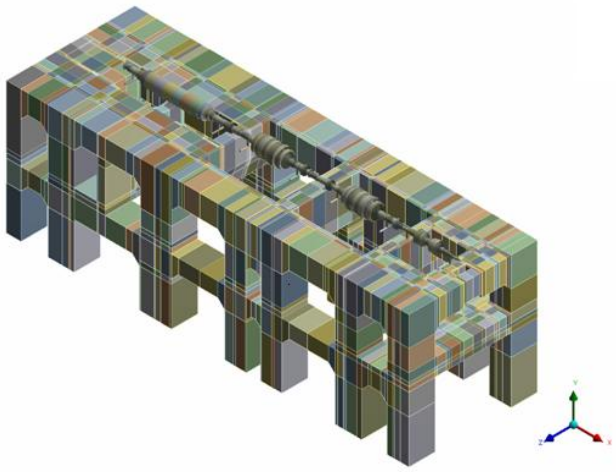

Figure 4. *3D geometric coupled model of the turbo-generator and the pedestal.*

For the numerical model of the turbo-generator type beam elements were used, settled geometric features of each section of the rotors according to their lengths, inner and outer diameters and the area of the cross section of each component, to reproduce its geometry as nearly as possible. It should be noted that the numerical model was developed using type beam elements, since the convergence of results in terms of modal shapes and natural frequencies between FEM model of the turbo-generator using 3D solid elements and other using beam type elements. In the Figure 5, is shown the numerical model of the turbo-generator.

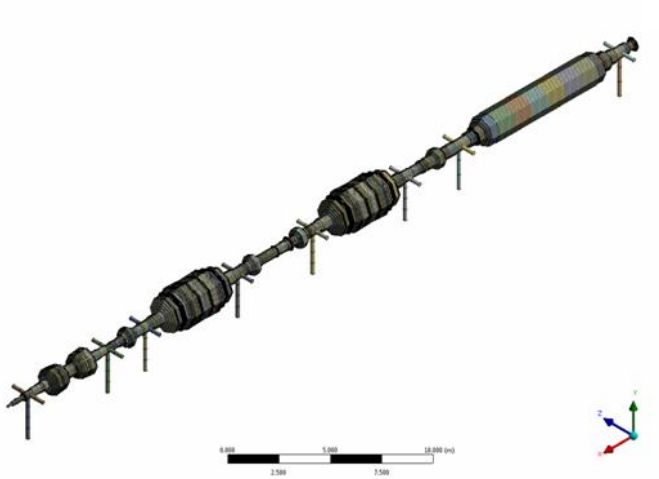

Figure 5. *Numerical model of the turbo-generator, using beam elements.*

The numerical model of the pedestal was developed using solid 3D elements of linear formulation [eight nodes] to model the simple concrete combined with the link type elements using to model the longitudinal steel reinforcement in the concrete columns and beams. Additionally, the element Revolute Joint is used to transmit the loads between the turbo-generator and the pedestal. Similar to be shown for the turbo-generator, in the Figure 6 is shown the numerical model of the reinforced concrete pedestal.

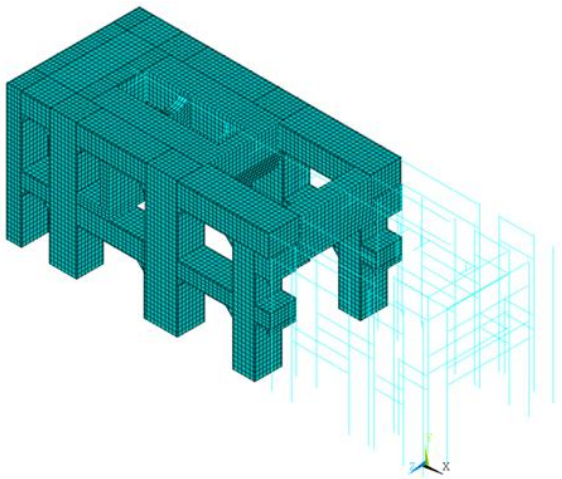

Figure 6. *Numerical model of the reinforced concrete pedestal.*

The coupled finite element model of the turbo-generator and reinforced concrete pedestal consists of 288,731 nodes and 71,240 elements in total.

Boundary Conditions

Boundary conditions of the coupled numerical model were established to restrict the displacements and translations of the pedestal on its three directions (x, y, and z) at the level of the foundation, as shown in the Figure 7.

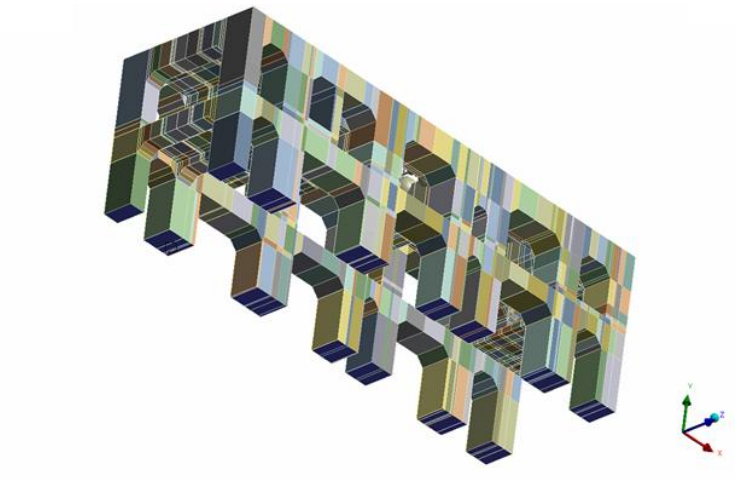

Figure 7. *Boundary conditions of the coupled numerical model.*

Materials Properties

The materials used in the manufacture of turbine rotors and electric generator consist of a NiCrMoV alloy steel, while the pedestal was designed with a material consisting of a resistant reinforced concrete compression (f'c) equal to 280 kg / cm^2 . Table 1, shows the types of materials for each rotor and the concrete pedestal, as well as some of its main mechanical properties [4, 5].

Table 1. Types of materials for each component

Component	Material		Properties				
			Modulus of Elasticity [Pa]	**Density [kg/m^3]**	**Poisson ratio**	**Yield strength [MPa]**	**Tensile strength [MPa]**
High Pressure Rotor	ST565S Class 2	23 CrNiMo 7-4-7	$2.03*10^{11}$	7,850	0.3	585	690
Low Pressure Rotors	ST565S Class 1	23 CrNiMo 7-4-7	$2.03*10^{11}$	7,850	0.3	635	740
Jack Shaft	ST573S	-	$2.03*10^{11}$	7,850	0.3	700	800
Electric Generator	-	27 NiCrMo 15-6	$2.03*10^{11}$	7,850	0.3	600	700
Pedestal	Concrete f'c = 280 kg/cm^2		$2.486*10^{10}$	2.325	0.17	-	-

Load Cases

During normal operation of the unit generation and according to their frequency of occurrence, two main types of load case can be induce damage to the pedestal; these load case include constant load or permanent actions, in addition to the repeated loads arising from the operation of the turbo-generator and their corresponding unbalance vibrations (oscillating loads).

Different load cases were defined based on reports by the manufacturer and are described below:

Permanents Loads

Gravitational Forces are applied at each support knowing weight of each component.

Torque Forces, in the case of the three turbines (LP1, LP2 and HP) are those for the reaction torque resulting from the static parts of the rotation of the turbine rotor (opposite in direction to the rotation of the rotor). For the case of electric generator is the resulting torque to the reaction of the magnetic field of the rotor on the stator windings.

Vacuum Forces are due that in the condenser of low pressure modules have a pressure less than atmospheric pressure.

Friction Forces these horizontal forces correspond to the thermal expansion of High Pressure, Low Pressure and Generator modules.

In the Figures 8 to 11, shows the different types of permanent loads acting on the concrete pedestal.

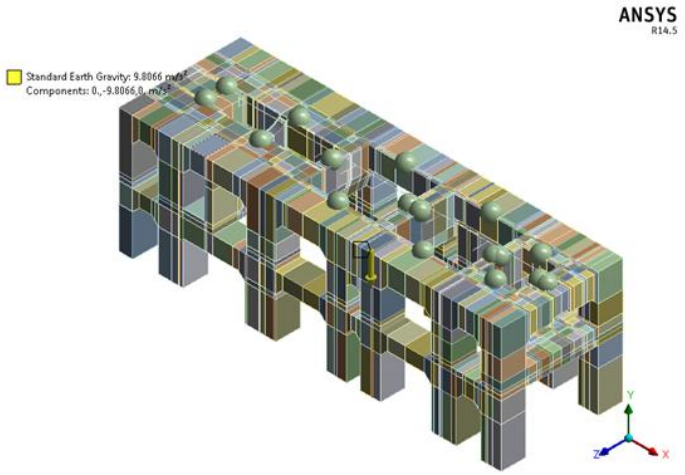

Figure 8. *Distribution of gravitational forces on the concrete pedestal.*

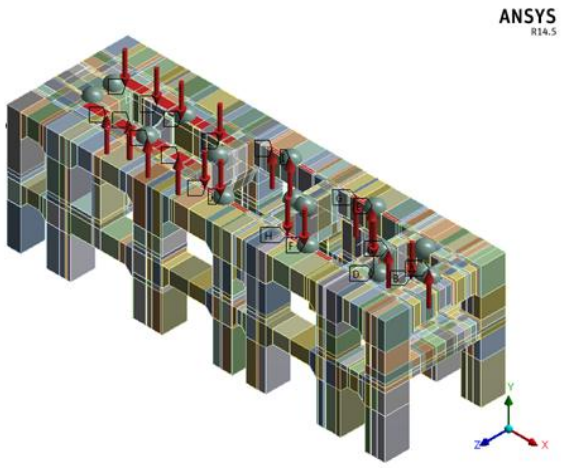

Figure 9. *Distribution of torque forces on the concrete pedestal.*

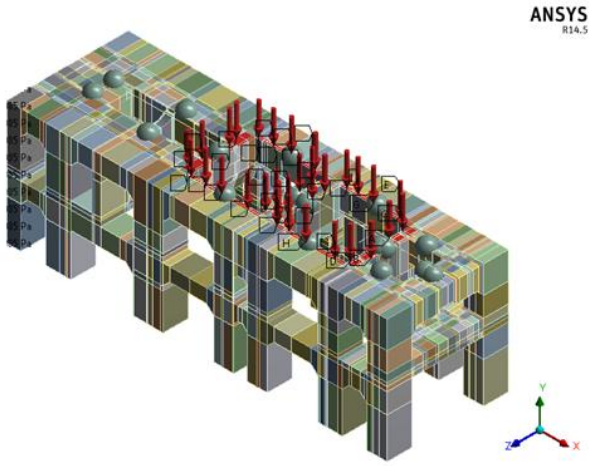

Figure 10. *Distribution of vacuum forces on the concrete pedestal.*

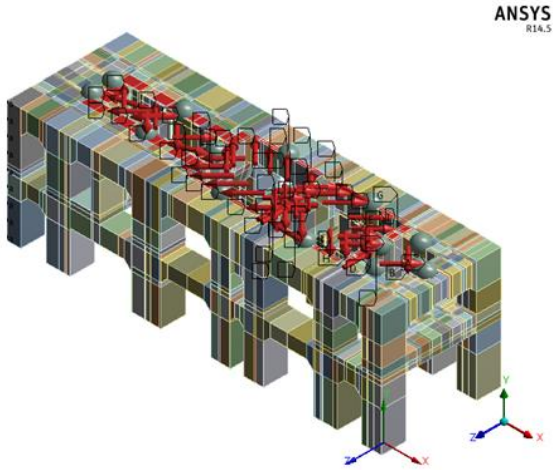

Figure 11. *Distribution of friction forces on the concrete pedestal.*

Oscillating loads

These conditions are important fluctuating loads generated by resonant vibratory phenomena either continuous or temporary; these resonance conditions are caused mainly by the turbo-generator unbalances that occur during normal operation due to the by vibration levels recorded in eight bearings that support the turbo-generator. The two different conditions of oscillating loads cases are described below.

Nominal Unbalance

This operational condition refers to existing vibrations in the turbo-generator at the nominal frequency operation of the generation unit, with resonant oscillations in the High Pressure Rotor (1ST mode) and the Rotor of the Electric Generator (2nd mode). These effects can be observed in the relative displacements measurements at real time in the bearings one and eight for the HP y GE Rotors as shown in Figure 12.

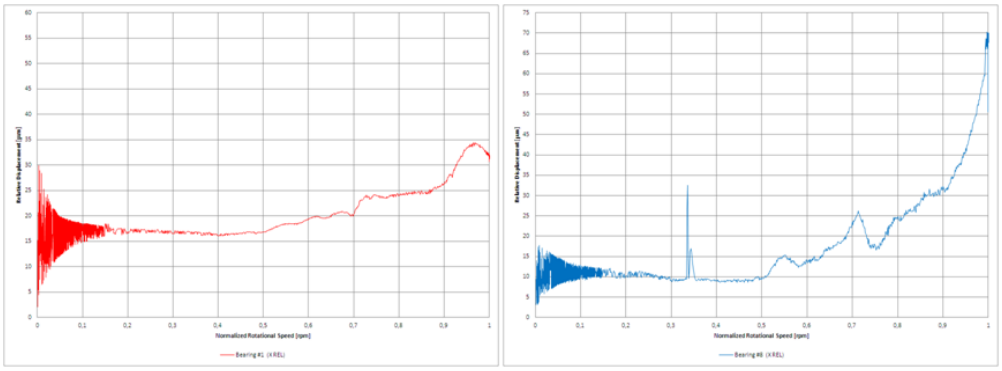

Figure 12. *Vibration data collection in two of eight turbo-generator bearings during a cold startup.*

This load case is developed by a dynamic analysis, which represents the maximum relative displacement peak to peak between the rotor and the bearings, equivalent to the alarm settings currently used for the real operation condition of the turbo-generator. This effect was developed assigning in the balancing planes for each rotor, harmonic forces that cause an unbalance in the turbo-generator as shown in Figure 13.

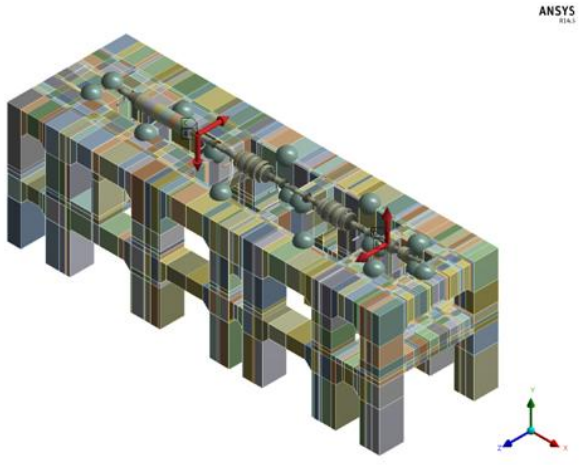

Figure 13. *Harmonic forces in the balancing planes for the HP and GE rotors.*

Startup and Shutdown

This operating condition is due to the unbalance of the rotors of Low Pressure and Electric Generator of the turbine, when they passage through its first critical speed for increased or decreased load on a process start or shutdown for the generation unit. This operational condition is not continuous and occurs only a few times each year. As in the case load of nominal unbalance, it is necessary to excite the numerical model until vibration limit on peak to peak at resonant frequencies for rotors of LP and GE. In the Figure 14, is shown the harmonic forces that cause an unbalance in these rotors.

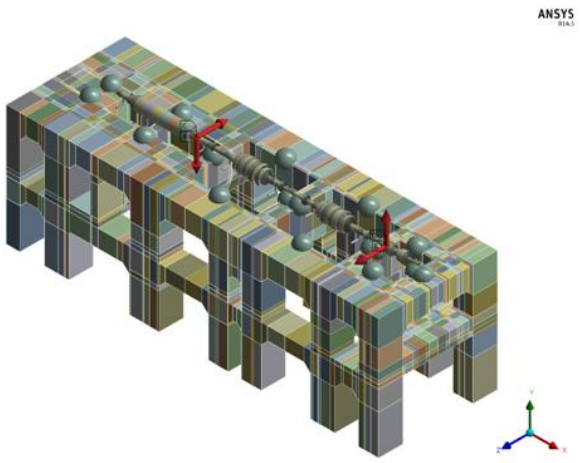

Figure 13. *Harmonic forces in the balancing planes for the LP and GE rotor during startup or shutdown.*

Numerical Results

In the numerical analysis of the structure the permanents loads remain during all time and are combined separately with each oscillating loads to determinate the dynamic behavior of the structure. The stress evaluation is presented for the nominal unbalance and the startup-shutdown conditions.

The Figure 14 is shown the numerical response of the Rotors of HP and GE (vertical and horizontal) at the nominal frequency operation of the generation unit for the nominal unbalance condition. Likewise, in the Figure 15 shows the critical zones and stress distribution in the reinforced concrete pedestal for nominal unbalance condition. Similarly, in the Figures 16 and 17 are shown the numerical response of the Rotors of LP and GE (vertical and horizontal) at the startup-shutdown condition. Likewise, in the Figures 18 and 19 are shown the critical zones and stress distribution in the reinforced concrete pedestal for this load condition.

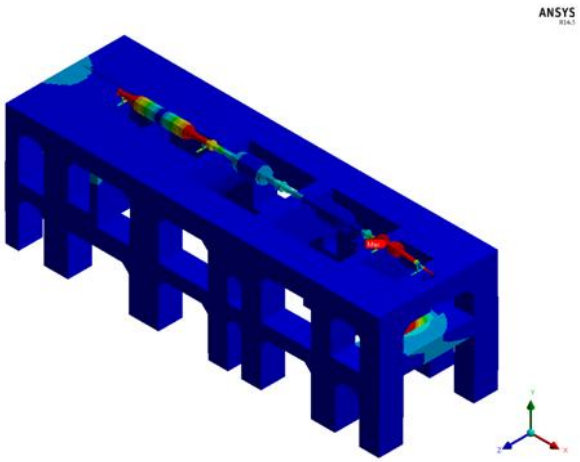

Figure 14. *Response of the Rotors of HP and GE at the nominal frequency operation of the generation unit for the nominal unbalance condition.*

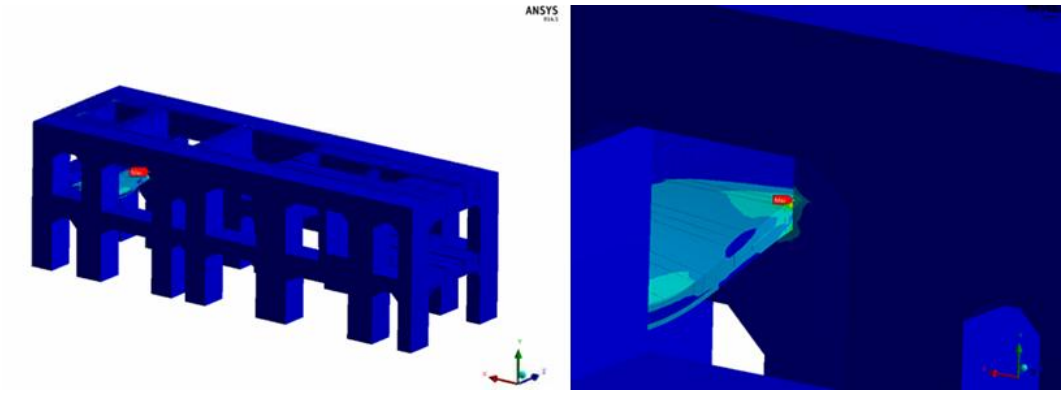

Figure 15. *Critical zones and stress distribution in the reinforced concrete pedestal for nominal unbalance condition.*

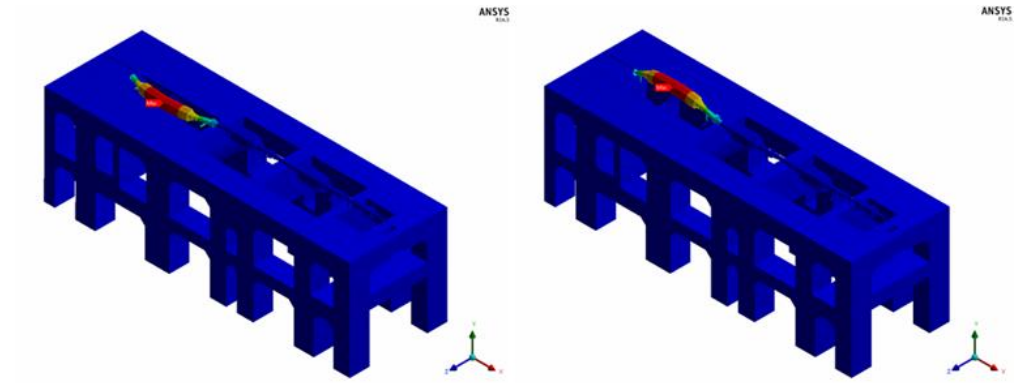

Figure 16. *Numerical response of the GE Rotor (vertical and horizontal) at the startup-shutdown condition.*

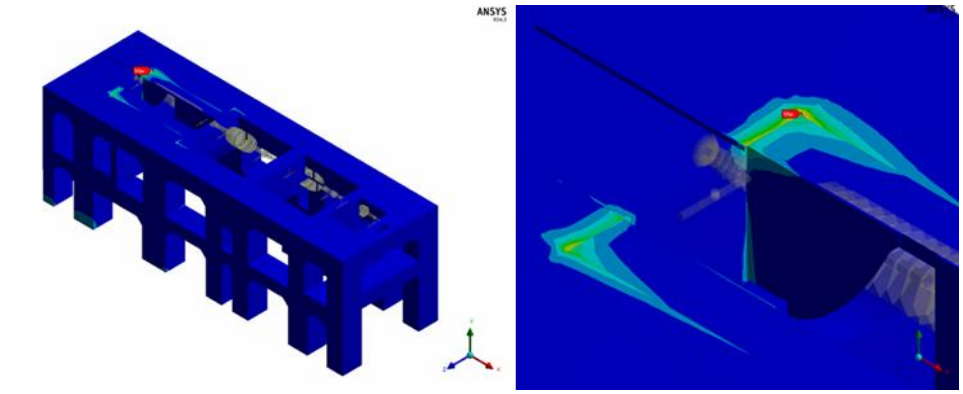

Figure 17. *Critical zones and stress distribution in the reinforced concrete pedestal for the startup-shutdown condition of the GE Rotor.*

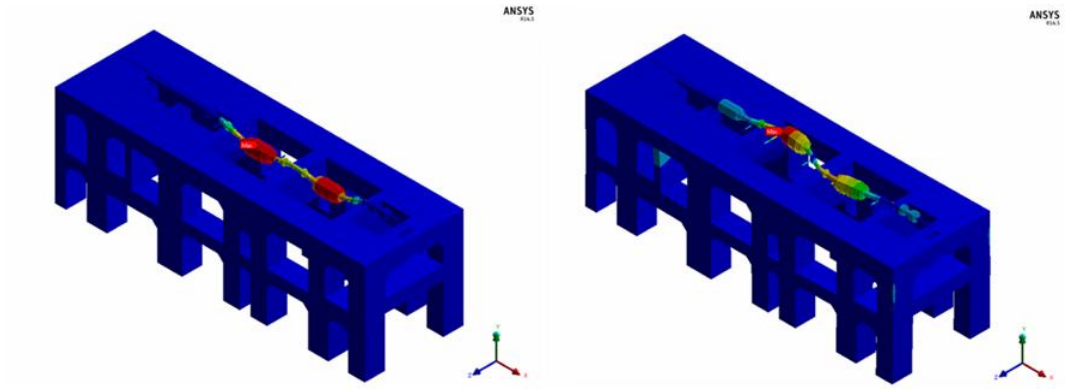

Figure 18. *Numerical response of the LP Rotors (vertical and horizontal) at the startup-shutdown condition.*

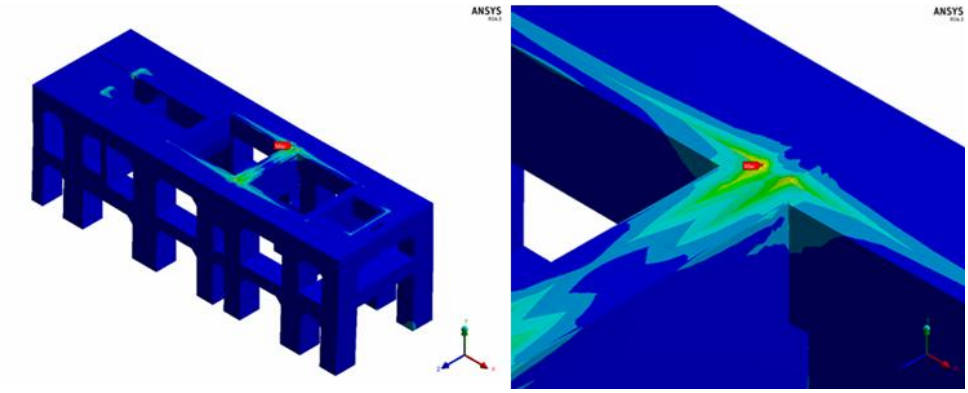

Figure 19. *Critical zones and stress distribution in the reinforced concrete pedestal for the startup-shutdown condition of the LP Rotors.*

4. DAMAGE ASSESSMENT OF THE STRUCTURE

A methodology for the study of fatigue of reinforced concrete elements subjected to high load cycles under the criteria of Stress-Life is presented. This approach is based on life curves called S-N (stress-number of cycles) obtained for alternating stresses in pure tension and compressive-tension stress, which determine the behavior of reinforced concrete using the nCode Design Life module for Ansys fatigue code.

High cycles criteria of damage assessment for the reinforced concrete pedestal was established, because the stress levels obtained in the dynamics evaluation of the structure are low and the behavior of the structure remains in the linear range. Also, the exposition time of the structure at these loads conditions is highest by its nature, which represents a phenomenon of high cycle's fatigue.

High cycle fatigue is controlled by the level of cyclic stress and uses an approach according to the equation Stress-Life (S-N) or Basquin equation [6], assumed that the failure occurs after a large number of cycles and shows the relationship between the stress amplitude about the failure, as shown in the following equation:

$$\frac{\sigma}{2} = \sigma_a = \grave{\sigma_f}\left(2N_f\right)^b \tag{1}$$

Where:

$\grave{\sigma_f}$, is the fatigue strength coefficient.

b, is the fatigue strength exponent

N_f, is the fatigue life.

σ_a, is the alternating stress.

The fatigue damage (d_i) can be defined as the ratio of load cycles (n_i)under certain operating conditions between the cycles of life of the component before failure$\left(N_f\right)$; such that the total accumulated damage in a component exposed to different loads conditions during normal operation according the high cycles fatigue uses the linear damage accumulation rule or Palmgren-Miner rule [7], which is a linear sum of individual damage induced to component for each load cycle during operation. This rule is denoted by the following expression:

$$D = \sum_{i=1}^{n} d_i \tag{2}$$

The failure occur when the sum of the damage for each operating condition or cumulative total damage of the material or greater than unit.

Fatigue Properties of Concrete

Recently, authors such as Lü et al [8] proposed a method to assess the fatigue under direct tension stresses and alternating compression-tension stresses on simple concrete, which is expressed by the following equations:

$$\log N = 12.02 - 10.64\left(\frac{\sigma_{max}}{f_t}\right) - 4.39\left(\frac{\sigma_{min}}{f_c}\right) \textit{for tension-compression stresses} \quad (3)$$

$$\log N = 16.67 - 16.76\left(\frac{\sigma_{max}}{f_t}\right) + 5.17\left(\frac{\sigma_{min}}{f_t}\right) \textit{for direct tension stresses} \quad (4)$$

Where:

σ_{max} , is the maximum stress.

σ_{min}, is the minimum stress.

f_c, is the compression stress.

f_t, is the tension stress.

R, is the stress ratio.

N, is the fatigue life.

Based on equation 1, 3, 4 and considering that the tensile stress of the reinforcing steel elements were 10.5 MPa, diverse SN curves were developed for the case alternating compression-tension stresses and direct tension stresses, varying the value of stress ratio R, as shown in Figure 20.

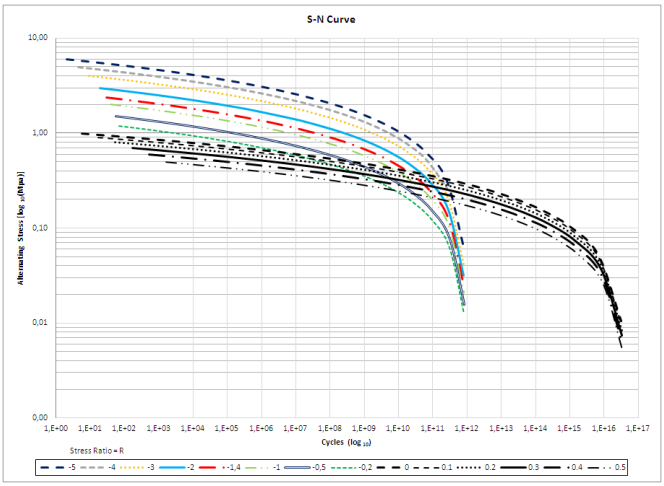

Figure 20. *S-N curves under direct tension stresses and tension-compression stresses for the pedestal.*

Fatigue Results

Based on the results from the evaluation of the dynamic behavior of the reinforced concrete pedestal, considering the criterion of high cycle fatigue S-N curves, the periods of occurrence of each load condition and the material properties of each column and beam which considered the inclusion of steel reinforcement; damage and life of the structure for each load condition are determined as well as a cumulative damage.

In the Figures 21 to 24, are shown the global distribution of life and damage for each load condition as well as the combination of them. In similar form for each condition and combination of loads, the Figures 25 to 28 shows the global distributions of damage to the reinforced concrete pedestal.

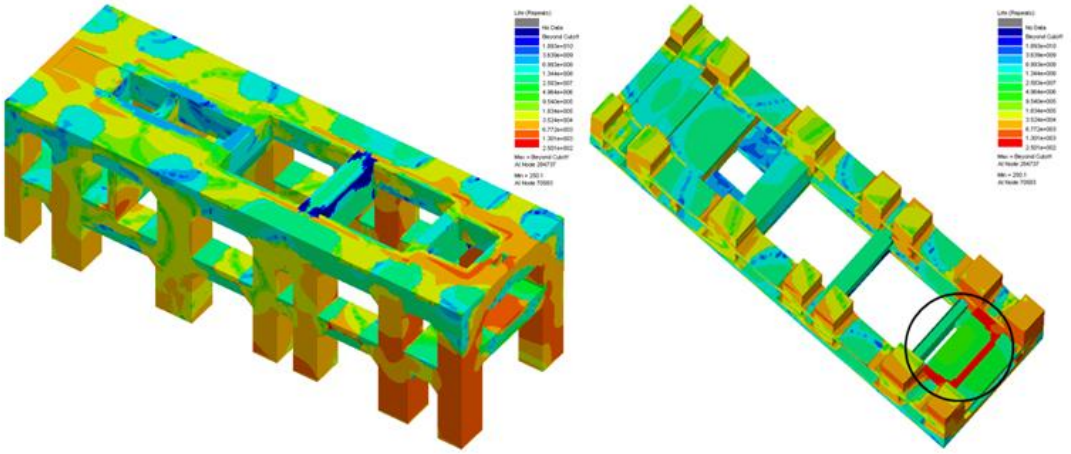

Figure 21. *Global distribution of life in the pedestal under nominal unbalance load condition.*

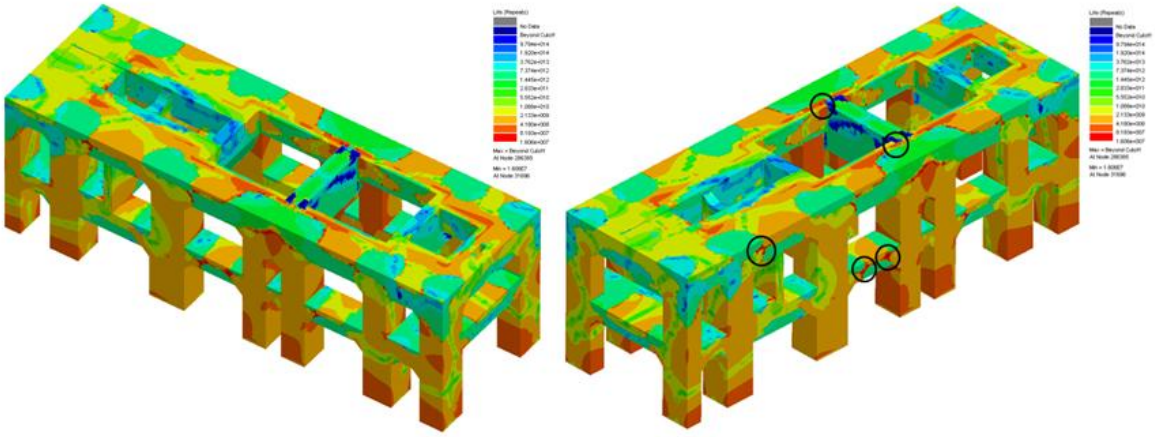

Figure 22. *Global distribution of life in the pedestal under LP startup-shutdown load condition.*

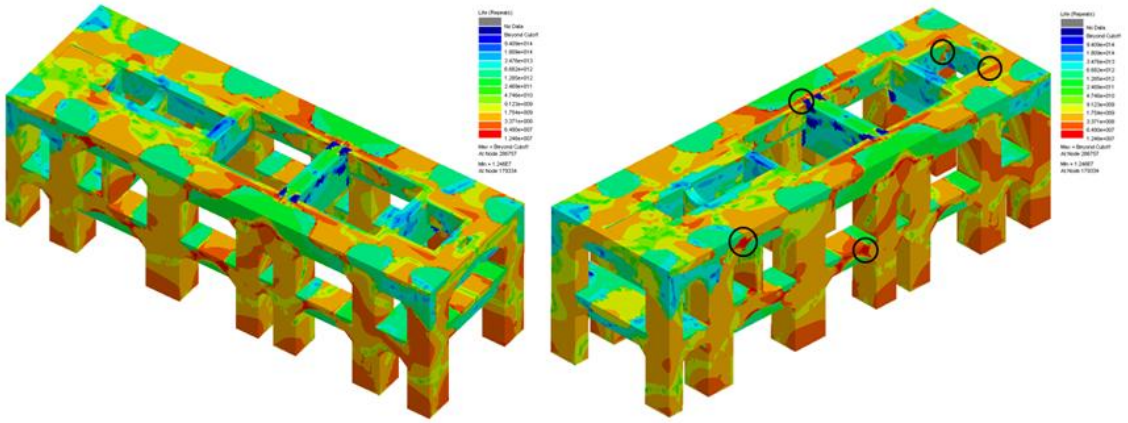

Figure 23. *Global distribution of life in the pedestal under GE startup-shutdown load condition.*

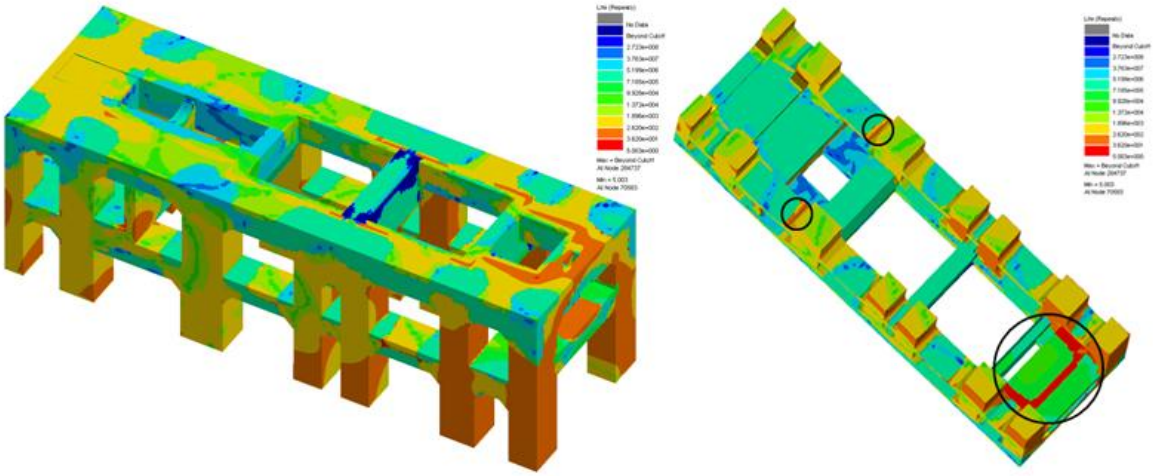

Figure 24. *Global distribution of life in the pedestal under the combination of load conditions.*

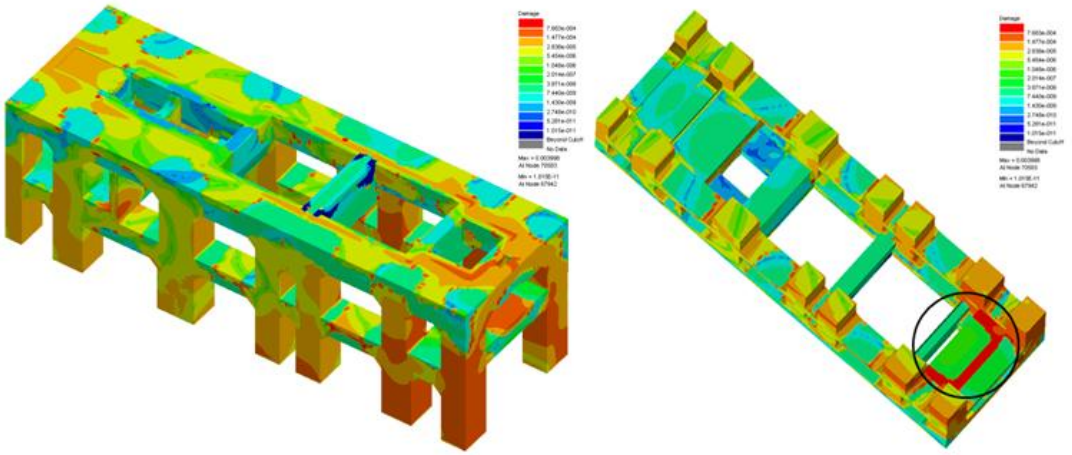

Figure 25. *Global distribution of damage in the pedestal under nominal unbalance load condition.*

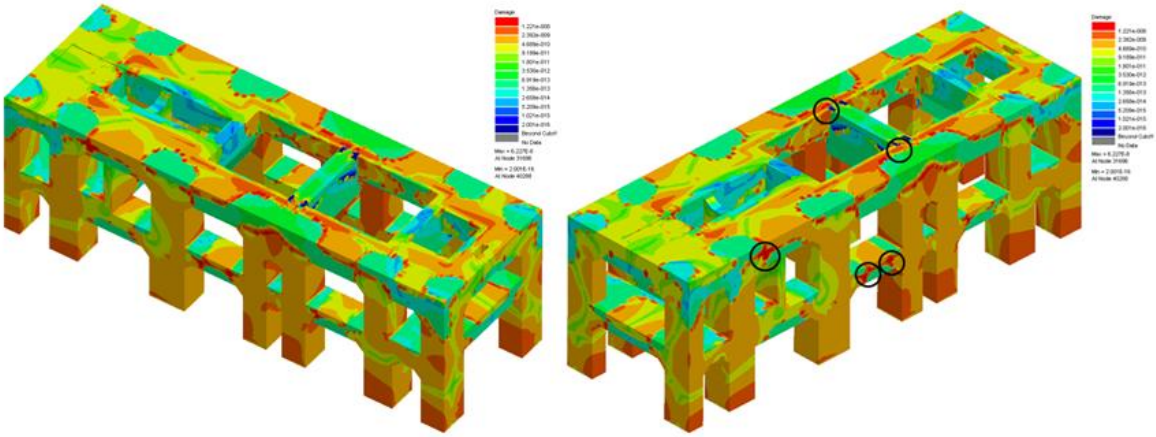

Figure 26. *Global distribution of damage in the pedestal under LP startup-shutdown load condition.*

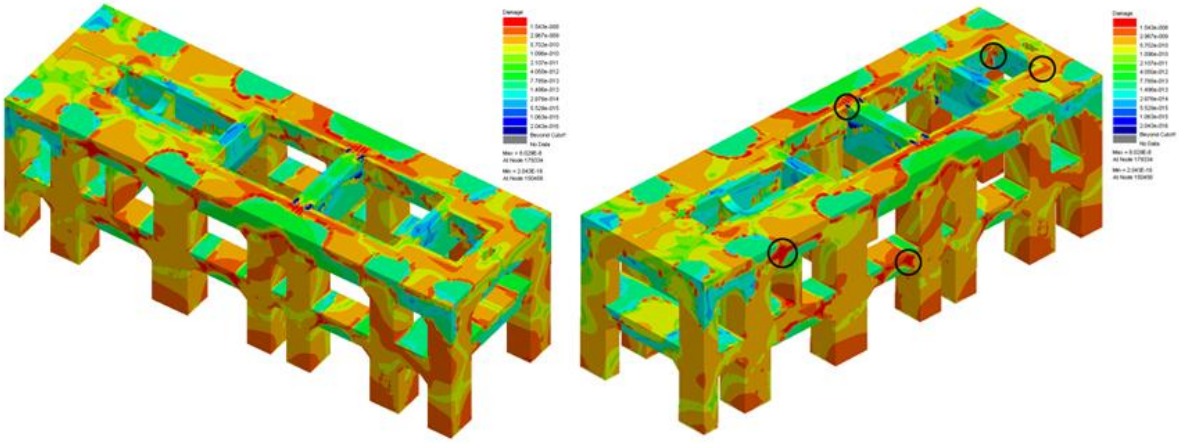

Figure 27. *Global distribution of damage in the pedestal under GE startup-shutdown load condition.*

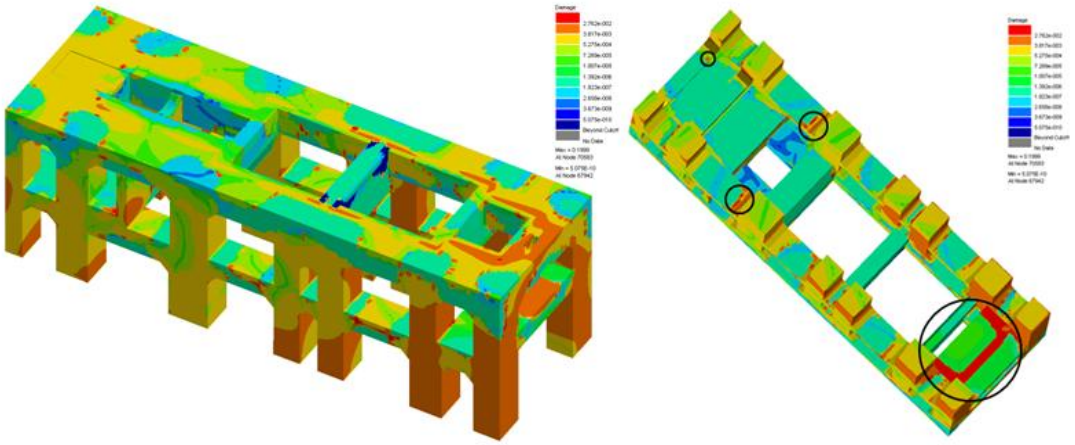

Figure 28. *Global distribution of damage in the pedestal under the combination of load conditions.*

5. CONCLUSIONS

New considerations on the methodology were implemented to assess the fatigue resistance of reinforced concrete in relation to the definition of the S-N Curves for reinforced concrete and its tensile stress. Also, were determine the critical zones to fatigue failure and an estimate of remaining fatigue life in the pedestal, which shows that after 50 years of service life consumption is 15.84 %. Then, 315 years of service are required to consume 100% of life in the pedestal. The dynamic behavior of the turbo-generator, as well as the remaining life in the pedestal can be improved if the stiffness levels of the bearings are modified in the high pressure rotor and electric generator.

It is important to consider that the cumulative damage will grow if other loading cases are presented as they would be, for example, an accidental unbalance in turbines or the seismic effect.

ACKNOWLEDGMENTS

The authors wish to express their thanks to the Electrical Research Institute (IIE) and The Federal Electricity Commission (CFE) for supporting this work.

REFERENCES

[1] General Foundations and Static and Dynamic Loads Transmitted to the Concrete Pedestal of the Turbine Unit - Retrofit Project, Federal Electricity Commission (CFE, in Spanish). 2010.

[2] Turbine, Frames and Equipment's Assembly Drawing - Retrofit Project, Federal Electricity Commission (CFE, in Spanish). 2010.

[3] ANSYS, User's Manual for Structural and dynamics Stress Analysis V14.5.

[4] Turbine Components Materials - Retrofit Project, Federal Electricity Commission (CFE, in Spanish). 2010.

[5] ASTM A471 / A471M. Standard Specification for Vacuum-Treated Alloy Steel Forgings for Turbine Rotor Disks and Wheels.

[6] Chai Y.H., Romstad K.M.(1996), "Characterization of structural damage under high-intensity seismic loading" , Elsevier Science Ltd, Eleventh World Conference on Earthquake Engineeering.

[7] M.A. Miner (1945). Cumulative damage in fatigue, p. A159-A-164. Transactions, American Society of Mechanical Engineering Vol. 67.

[8] P. Lü, Q. Li and Y Song (2004). Damage constitutive of concrete under uniaxial alternate tension-compression fatigue loading based on double bounding surfaces, p. 3151-3166. Elsevier Ltd., International journal of solids and structures, Vol. 41.